PROCEEDINGS OF SCIENCE

On the origin of gamma-ray emission toward SNR CTB 37A with *Fermi*-LAT

S. Abdollahi * †
Department of Physical Sciences, Hiroshima University, Higashi-Hiroshima, Hiroshima 739-8526, Japan
E-mail: soheila@astro.hiroshima-u.ac.jp

T. Mizuno
Hiroshima Astrophysical Science Center, Hiroshima University, Higashi-Hiroshima, Hiroshima 739-8526, Japan
E-mail: Mizuno@astro.hiroshima-u.ac.jp

Y. Fukazawa
Department of Physical Sciences, Hiroshima University, Higashi-Hiroshima, Hiroshima 739-8526, Japan
E-mail: fukazawa@astro.hiroshima-u.ac.jp

H. Katagiri
College of Science, Ibaraki University, 2-1-1, Bunkyo, Mito 310-8512, Japan
E-mail: hideaki.katagiri.sci@vc.ibaraki.ac.jp

B. Condon
Centre d'Études Nucléaires de Bordeaux Gradignan, IN2P3/CNRS, Université Bordeaux 1, BP120, F-33175 Gradignan Cedex, France
E-mail: condon@cenbg.in2p3.fr

Supernova remnants (SNRs) are believed to be one of the major sources of Galactic cosmic rays. SNR CTB 37A is known to interact with several dense molecular clouds as traced by OH 1720 MHz maser. Radio and X-ray observations of the SNR confirm a mixed-morphology classification of the remnant. The TeV γ-ray source HESS J1714-385 is positionally coincident with the SNR, though it is still not clear whether the TeV γ-ray emission originates in the SNR or a plausible pulsar wind nebula (PWN). In the present work, we use 8 years of Pass 8 *Fermi*-LAT data, with high capability to resolve γ-ray sources, to perform morphological and spectral studies of the γ-ray emission toward CTB 37A from 200 MeV to 200 GeV. The best fit of the source extension is obtained for a Gaussian model of 68% containment radius $0.18^\circ \pm 0.02^\circ$. We also discuss several possible theoretical models to explain the broadband spectrum and to elucidate the nature of the high-energy γ-ray emission toward CTB 37A.

35th International Cosmic Ray Conference ICRC 2017,
10-20 July, 2017
Bexco, Busan, Korea

*Speaker.
†On behalf of the *Fermi*-LAT collaboration

PoS(ICRC2017)743

1. Introduction

The *Fermi*-LAT survey of the Galactic plane has detected dozens of supernova remnants (SNRs) which are promising candidates for emission of Galactic cosmic rays at least up to energies of 10^{15} eV [1]. Non-thermal multi-wavelength emission from SNRs in radio, X-rays and very high energy (VHE) γ-rays (E > 100 GeV) arises from a population of relativistic particles accelerated in the SNR shock front interacting with the surrounding medium (see, e.g., [1, 2]). X-ray synchrotron emission from extremely energetic electrons at the shock front up to $\sim$ 100 TeV was first observed in the remnant of SN 1006 [3] and then in a dozen young SNRs including Cassiopeia A [4], Vela Jr. [5], RX J1713.7-3964 [6], and G1.9+0.3 [7]. A number of SNRs have recently been identified in the GeV and/or TeV energy range. The origin of γ-ray emission from the SNRs can be leptonic processes (via inverse Compton scattering of cosmic microwave background or non-thermal bremsstrahlung), or hadronic processes (via decay of π^0 mesons produced in inelastic proton-proton collisions).

The characteristic decrement of γ-ray emission below $\sim$ 200 MeV (often called *pion bump*) in the middle-aged SNRs IC443 and W44 associated with molecular clouds, confirmed by the *Fermi*-LAT [8], is explicitly linked to the hadronic acceleration. Additional evidence for a hadronic origin of γ-ray emission from relatively old SNRs interacting with molecular clouds comes from observations of W51C, W28, W41, MSH 17-39, G337.7-0.1, and G5.7-0.1.

CTB 37A (also known as G348.5+0.1), first identified in radio surveys [9], is a middle-aged SNR associated with nearby dense molecular clouds in an inhomogeneous region as evidenced by OH 1720 MHz masers detected towards the remnant [10] and shocked clumps of clouds with high column densities [11]. It is a mixed-morphology SNR [12], characterized by center-filled thermal X-ray emission surrounded by a shell-like radio structure. The distance of CTB 37A is estimated to be 9.5 kpc using a measurement of H I absorption at 21-cm [13]. Previously, from velocity measurement of molecular clouds associated with the remnant, the distance had been determined to be 11.3 kpc [11]. CTB 37A is located in the complex region of CTB 37 which contains the SNR CTB 37B (G348.7+0.3, associated with HESS J1713-381) and SNR G348.5-0.0 as well. CTB 37A has been observed extensively across a wide range of energies from radio to VHE γ-rays. Radio observations of the SNR reveal a shell-like structure in the north plus a breakout morphology extending to the south. In the X-ray band, in addition to the soft thermal emission, extended non-thermal hard X-ray emission has been detected from the remnant, indicating the emission from a pulsar wind nebula [12, 14]. The TeV γ-ray source HESS J1714-385 is positionally coincident with the SNR, though the leptonic or hadronic nature of γ-ray emission toward this source is still under debate [12]. Deeper observations of the region of CTB 37A, especially in the GeV band, provide new insights on the origin of the γ-ray emission coincident with the SNR.

In this proceeding, we present a summary of the detailed analysis of CTB 37A using 8 years of *Fermi*-LAT Pass 8 data, and discuss the spatial extension and spectral characterization of the γ-ray emission toward the remnant, which are crucial for distinguishing between hadronic and leptonic scenarios. In Section 2, observation and data reduction are described. The analysis procedures and results are given in Section 3, where the morphological and spectral analysis of CTB 37A is explained. In Section 4, the modeling of the broadband spectrum is discussed. More detailed analysis and discussion will be presented in a future publication.

2. Observation and Data Reduction

The Large Area Telescope (LAT) on board the *Fermi* Gamma-ray Space Telescope is a pair-conversion γ-ray detector covering the energy range from about 20 MeV to above 300 GeV. The LAT is equipped with a tracker/converter for direction reconstruction, a CsI hodoscopic calorimeter for measurement of the energy deposition, and an Anti-Coincidence Detector (ACD) for charged particle background rejection. Full details of LAT instrument and data processing can be found in [15], and information regarding the on-orbit calibration is given in [16]. Relative to earlier gamma-ray missions, the LAT has a large effective area ($\sim$ 8000 cm^2 on-axis for above 1 GeV), a wide field of view ($\sim$ 2.4 sr at 1 GeV), and improved point-spread function (PSF; the 68% containment angle above 1 GeV is smaller than 1°).

The LAT data used for the following analysis were collected during the first 8 years of scientific operations, which began on 2008 August 4. The γ-rays in the energy range 200 MeV$-$200 GeV within a region of interest (ROI) of radius 15° centered on the position of CTB 37A are selected for the analysis. The event selection is based on the "Pass 8 source" event class (corresponding `P8R2_SOURCE_V6` instrument response functions (IRFs)), and a zenith angle cut of 105° and 90° for events above and below 1 GeV, respectively, is applied to reduce the contamination from the Earth limb. The selected 200 MeV lower limit is to avoid challenges in spectral analysis below that energy because of large uncertainties in diffuse emission models at low energies and the rapid change of effective area with energy.

3. Analysis and Results

Two different software packages, `gtlike` and `pointlike`, were used to perform the spatial and spectral analyses. `gtlike` is a standard tool for maximum-likelihood fitting [17], implemented in the Science Tools distributed publicly by the *Fermi* Science Support Center. `pointlike` is an alternative tool to perform binned-likelihood analysis, optimized to localize the source and to characterize its extension, and has been tested extensively against `gtlike` [18, 19]. These tools fit a source model to the LAT data along with models for the instrumental, extragalactic and Galactic components of the background.

In the following analysis, the Galactic diffuse emission model *gll_iem_v06.fits* and isotropic diffuse model *iso_P8R2_SOURCE_V6_v06.txt* were used in the source model. In addition, all background sources within 20° around CTB 37A reported in the 3rd *Fermi*-LAT catalog (3FGL) [20] and also CTB 37B (3FHL J1714.0-3811) located in the vicinity of CTB 37A are included. CTB 37B has been resolved recently by the LAT at energies above 10 GeV [21]. Background sources are considered over an area 5° larger than the ROI to account for the contamination from those sources. The source model is used for the binned likelihood analysis by combining four P8R2 SOURCE V6 PSF event types in a joint likelihood technique. In the first step, for the morphological analysis, the flux normalizations and spectral indices of all 3FGL sources within 5° of the ROI center and the normalizations of the Galactic and isotropic components are free to vary over the entire energy range from 200 MeV to 200 GeV, while the spectral parameters of other sources are fixed at the 3FGL values. Then to measure the energy spectrum of CTB 37A, γ-ray data are fit to the model in narrow energy bins with all parameters except the normalization of the diffuse components and that

Table 1: Results of localization and extension fits with `pointlike` using all events in the 0.2-200 GeV energy range. TS_{ext} is the test statistic of the extended source model over the point source model, and α is the spectral index of the LogParabola model. E_b and β of the model are fixed (see text for details).

Spatial Model	R.A. (°)	Dec. (°)	r_{68} (°)	TS_{ext}	Spectral Index (α)
Point Source	258.65±0.01	-38.54±0.01			2.13±0.01
Disk	258.68±0.01	-38.56±0.01	0.17±0.01	138.54	2.057±0.003
Gaussian	258.67±0.01	-38.55±0.01	0.18±0.02	145.69	2.04±0.01

of CTB 37A, CTB 37B, and the very bright γ-ray source RX J1713.7-3946 (which is located at a distance of $\sim$1.23° from CTB 37A) are fixed to those previously found in the overall fit. Fixing the spectral parameters to those obtained in the overall fit helps with avoiding numerical instabilities resulting from the fine binning in energy.

Uncertainties associated with the modeling of interstellar diffuse emission and the LAT IRFs are the main sources of systematic error. In this contribution, we give statistical errors only and will discuss on the systematic uncertainties in a future publication.

3.1 Morphological Analysis

The spatial analysis of the source was performed using all events in the energy range $0.2-200$ GeV. The position and possible spatial extension of CTB 37A were determined using `pointlike` assuming a LogParabola spectral shape, $F(E) = \Phi_0(E/E_b)^{-(\alpha+\beta log(E/E_b))}$, as described in the 3FGL. Using a point-like spatial model, the best-fit position of the source in equatorial coordinates is (Right Ascension (R.A.), Declination (Dec.)) = (258.65°±0.01°, -38.54°±0.01°), which is consistent with the position in the 3FGL, within uncertainties.

To examine the possible source extension, CTB 37A was also modeled using two spatial hypotheses, a Gaussian distribution and a uniform disk. The resulting spatial and spectral parameters are summarized in Table 1. TS_{ext} is defined as $2\times(\mathcal{L}_{\rm extended}\text{-}\mathcal{L}_{\rm point})$ where the expression in parentheses is the log-likelihood difference between extended and point source models. r_{68} is the 68% containment radius, and α is the index in the LogParabola spectral model. The LogParabola curvature (β) and energy reference (E_b) are fixed to the 3FGL values of 0.12 and 1.11 GeV, respectively. According to the results, the best spatial model is a Gaussian distribution with $\sigma = 0.12° \pm 0.01°$, which is equivalent to a source size of $r_{68} = 0.18° \pm 0.02°$ and in good agreement with the previously reported value based on 6 years data [22].

Figure 1 shows the LAT counts map (left) and test statistic (TS) map of CTB 37A in the 0.2-200 GeV energy range (right). The positions of two bright sources in the TeV and X-ray bands are marked by a red cross and a black diamond on the TS map. MOST 843 MHz Radio (green) and Chandra X-ray (cyan) contours are shown in addition to the source extension size of CTB 37A (blue circle). As can be seen, the source size in the GeV band is comparable with that in the radio [23].

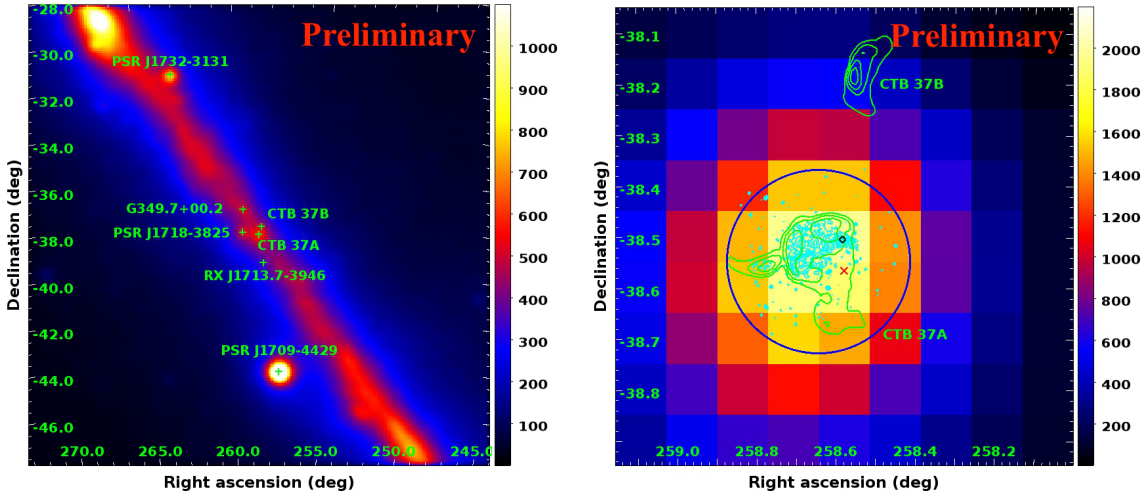

Figure 1: (Left): *Fermi*-LAT counts map in 0.2-200 GeV around SNR CTB 37A with a pixel size of 0.1° smoothed with a Gaussian kernel of 0.15°, (Right): TS excess map of CTB 37A in 0.2-200 GeV. The 843 MHz radio contours from MOST are overlaid in green, and the X-ray contours from Chandra are shown in cyan. The position of HESS J1714-385 is marked with a red cross. The black diamond indicates the position of the X-ray source CXOU J171419.8-383023. The 68% containment radius obtained by the Gaussian spatial model is shown with a blue circle.

3.2 Spectral Analysis

Since CTB 37A is significantly extended, we produce its spectral energy distribution (SED) with a Gaussian spatial distribution. The spectral analysis was performed with `gtlike` using all events between 200 MeV and 200 GeV. The energy range was divided into 9 logarithmically spaced energy bins; however, no significant emission from the source was detected at energies above $\sim$ 100 GeV. A power law with the spectral index fixed at 2.0 in each energy bin is used to model the spectrum. First, a source model with 5 degrees of freedom (2 for normalization of diffuse components and 3 for that of CTB 37A, CTB 37B, and RX J1713.7-3946) was used to represent the γ-ray emission within the ROI. However, the residual map reveals significant negative excess at the position of J1726.6-3530c at low energies. To account for the negative residuals at this position, the normalization and index of that source were also left free. We note that the modified model improves the fit by removing the residuals but does not significantly affect the spectrum of CTB 37A. Figure 2 shows the γ-ray spectrum of CTB 37A, where a statistical upper limit is calculated when the detection is not significant (TS < 4). The total γ-ray energy flux of CTB 37A in the 0.2-100 GeV energy range is calculated to be (90.54 ± 2.83) eV cm^{-2} s^{-1} and the photon flux is $(6.97 \pm 0.60) \times 10^{-8}$ ph cm^{-2} s^{-1}, where errors are only statistical. As can be seen in Figure 2, an extrapolation of the TeV spectrum slightly underpredicts the GeV flux, suggesting that two or more populations of the particle are responsible for the origin of the GeV and TeV emission.

4. Discussion

To identify the nature of γ-ray emission toward SNR CTB 37A and possible emission pro-

cesses, broadband modeling of the nonthermal emission from radio to VHE γ-rays is crucial. In the previous work [24], a mixed leptonic-hadronic model was used for the SED modeling of CTB 37A. Here, as a first step, we try to explain the γ-ray emission using a one-zone hadronic or leptonic scenario.

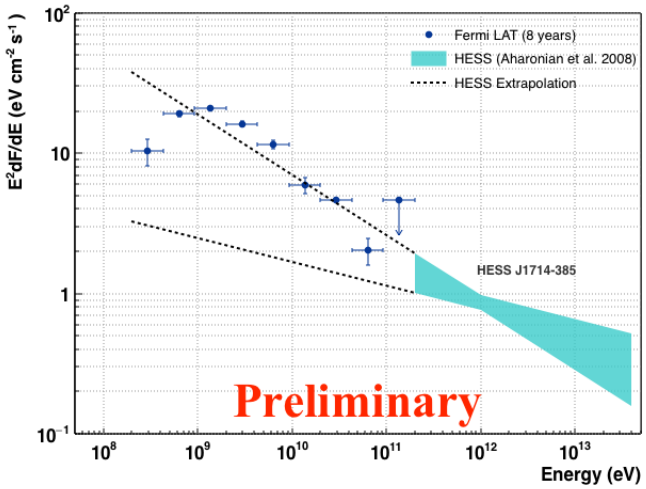

Figure 2: The γ-ray spectrum of CTB 37A obtained by *Fermi*-LAT. The shaded region denotes HESS J1714-385 measurements with statistical errors. Horizontal bars for *Fermi*-LAT data points indicate the energy range used in the fit and vertical bars show statistical errors. An upper limit is obtained where the TS is less than 4. The HESS spectrum is extrapolated to lower energies.

The presence of several dense molecular clouds close to the SNR and associated OH masers with VHE γ-ray emission support the hadronic scenario. However, the power law injection spectrum of protons with a spectral index of 2.71 can not connect to the TeV spectrum of HESS 1714-385 smoothly (see the top panel of Figure 3). In the case of the leptonic scenario, one possibility is that both X-rays and TeV γ-rays are produced by the same particle population (electrons) via synchrotron and inverse Compton processes. Therefore, magnetic field and interstellar radiation fields (ISRFs) are considered as key parameters; we assumed the magnetic field to be 10 μG (a typical

Table 2: One-zone models parameters.

Model	Parameters						Energetics	
	k_{ep}	Index$_1$	Index$_2$	E$_b$ (GeV)	B (μG)	n_H (cm^{-3})	W$_p$ (10^{49} erg)	W$_e$ (10^{47} erg)
Hadron-dominant (power law: PL)	0.01	2.70		8 .0		1095	1.27	
Lepton-dominant (PLSuperExpCutoff)	1.0	2.15	1.0		10	1095		2.75

Note: k_{ep} is the electron to proton ratio at 1 GeV. Index$_1$, Index$_2$, and the reference energy E$_b$ refer to spectral parameters. n_H is the average hydrogen number density of the ambient medium. W$_p$ and W$_e$ represent the total energy of protons and electrons, respectively.

value for middle-aged SNRs) and referred to [25] to model the optical and infrared ISRFs. The result obtained by Suzaku is adopted in X-ray band. We found that the VLA data and HESS TeV emission are underestimated by our model due to the strong constraint in the X-ray band, as seen in the bottom panel of Figure 3. The parameters of the one-zone hadronic and leptonic scenario are summarized in Table 2. The results show that it is crucial to study multi-zone models in order to understand the nature of the γ-ray emission toward the SNR.

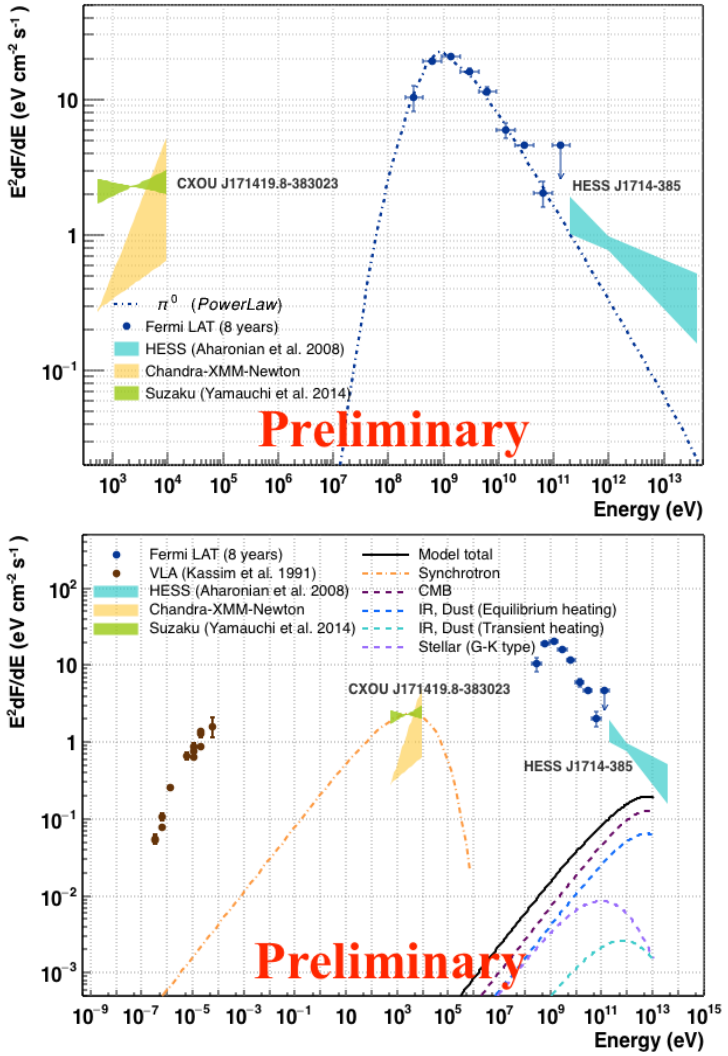

Figure 3: The one-zone hadronic model with the power law proton injection spectrum (top), and the leptonic model with injection spectrum of power law with super exponential cutoff (bottom). The VLA radio data and both Chandra-XMM and Suzaku X-ray spectra are indicated along with the HESS measurement.

5. Acknowledgments

The *Fermi*-LAT Collaboration acknowledges support for LAT development, operation and data analysis from NASA and DOE (United States), CEA/Irfu and IN2P3/CNRS (France), ASI

and INFN (Italy), MEXT, KEK, and JAXA (Japan), and the K.A. Wallenberg Foundation, the Swedish Research Council and the National Space Board (Sweden). Science analysis support in the operations phase from INAF (Italy) and CNES (France) is also gratefully acknowledged. This work performed in part under DOE Contract DE-AC02-76SF00515.

References

[1] J.A. Hinton and W. Hofmann, *Annual Review of Astronomy & Astrophysics* **47** (2009) 523-565

[2] F. A. Aharonian, *Astroparticle Physics* **43** (2013) 71-80

[3] K. Koyama et al., *Nature* **378** (1995) 255-258

[4] G. E. Allen et al., *Astrophysical Journal Letters* **487** (1997) L97

[5] P. Slane et al., *Astrophysical Journal* **548** (2001) 814-819

[6] Y. Uchiyama et al., *Nature* **449** (2007) 576-578

[7] S. P. Reynolds et al., *Astrophysical Journal Letters* **680** (2008) L41-L44

[8] M. Ackermann et al., *Science* **339** (2013) 807-811

[9] D. H. Clark et al., *Australian Journal of Physics, Astrophysical Supplement* **37** (1975) 1-38

[10] D. A. Frail et al., *Astronomical Journal* **111** (1996) 1651

[11] E. M. Reynoso et al., *Astrophysical Journal* **545** (2000) 874-884

[12] F. Aharonian et al., *Astronomy and Astrophysics* **490** (2008) 685-693

[13] W. W. Tian et al., *Monthly Notices of the Royal Astronomical Society* **421** (2012) 2593-2597

[14] S. Yamauchi et al., *PASJ* **66** (2014) 2

[15] W. B. Atwood et al., *Astrophysical Journal* **697** (2009) 1071

[16] A. A. Abdo et al., *Astroparticle Physics* **32** (2009) 193-219

[17] J. R. Mattox et al., *Astrophysical Journal* **461** (1996) 396-407

[18] M. Kerr, *Ph.D. Thesis, Univ. of Washington, Seattle, USA*, (2011) [arXiv:1101.6072v1]

[19] J. Lande et al., *Astrophysical Journal* **756** (2012) 5

[20] F. Acero et al., *Astrophysical Journal Supplement Series* **218** (2015) 23

[21] The *Fermi-LAT* Collaboration, (2017) [arXiv:1702.00664]

[22] J. Li et al., *Astrophysical Journal* **835** (2017) 30

[23] T. G. Pannuti et al., *Astronomical Journal* **147** (2014) 55

[24] T. J. Brandt et al., *Advances in Space Research* **51** (2013) 247

[25] A. W. Strong et al., *Astrophysical Journal* **537** (2000) 763